

The Geological Society Books

Chapter 4.1a Antarctic Peninsula I. Volcanology

--Manuscript Draft--

Manuscript Number:	GSLBooks18-059
Full Title:	Chapter 4.1a Antarctic Peninsula I. Volcanology
Article Type:	Chapter
Corresponding Author:	John Laidlaw Smellie University of Leicester Leicester, Leicestershire UNITED KINGDOM
Other Authors:	Malcolm Hole
Section/Category:	Volcanism in Antarctica: 200 Million Years of Subduction, Rifting and Continental Break-Up
Abstract:	<p>The Antarctic Peninsula is distinguished by late Neogene volcanic activity related to a series of northerly-younging ridge crest—trench collisions and the progressive opening of 'no-slab windows' in the subjacent mantle. The outcrops were amongst the last to be discovered in the region, with many occurrences not visited until the 1970's and 1980's. The volcanism consists of several monogenetic volcanic fields and small isolated centres. It is sodic alkaline to tholeiitic in composition and ranges in age between 7.7 Ma and present. No eruptions have been observed (with the possible, but dubious, exception of Seal Nunataks in 1893), but very young isotopic ages for some outcrops suggest that future eruptions are a possibility. The eruptions were overwhelmingly glaciovolcanic and the outcrops have been a major source of information on glaciovolcano construction. They have also been highly instrumental in advancing our understanding of the configuration of the Plio-Pleistocene Antarctic Peninsula Ice Sheet. However, our knowledge is hindered by a paucity of modern, precise isotopic ages. In particular, there is no obvious relationship between the age of ridge crest—trench collisions and the timing of slab-window volcanism, a puzzle that may only be resolved by new dating.</p>

1 **4. Post-subduction, slab-window volcanism**2 **Chapter 4.1a Antarctic Peninsula I. Volcanology**3 Smellie, J.L.¹ and Hole, M.J.²4 ¹*School of Geography, Geology and the Environment, University of Leicester, LE1 7RH, UK*5 ²*Department of Geology, University of Aberdeen, AB24 3UE, UK*6 **Abstract**

7 The Antarctic Peninsula is distinguished by late Neogene volcanic activity related to a series
8 of northerly-younging ridge crest—trench collisions and the progressive opening of ‘no-slab
9 windows’ in the subjacent mantle. The outcrops were amongst the last to be discovered in
10 the region, with many occurrences not visited until the 1970’s and 1980’s. The volcanism
11 consists of several monogenetic volcanic fields and small isolated centres. It is sodic alkaline
12 to tholeiitic in composition and ranges in age between 7.7 Ma and present. No eruptions
13 have been observed (with the possible, but dubious, exception of Seal Nunataks in 1893),
14 but very young isotopic ages for some outcrops suggest that future eruptions are a
15 possibility. The eruptions were overwhelmingly glaciovolcanic and the outcrops have been a
16 major source of information on glaciovolcano construction. They have also been highly
17 instrumental in advancing our understanding of the configuration of the Plio-Pleistocene
18 Antarctic Peninsula Ice Sheet. However, our knowledge is hindered by a paucity of modern,
19 precise isotopic ages. In particular, there is no obvious relationship between the age of ridge
20 crest—trench collisions and the timing of slab-window volcanism, a puzzle that may only be
21 resolved by new dating.

22

23 Introduction

24 Post-subduction volcanism occurred in the Antarctic Peninsula as a result of a series of
25 collisions between segments of an oceanic spreading centre and the Antarctic Peninsula
26 trench (Barker, 1982; Fig. 1). The collisions took place at progressively younger times from
27 south to north between c. 50 and 4 Ma. They caused the locking of the spreading centre at
28 the trench but continued subduction of the detached leading plate resulted in the opening
29 up of extensive 'no-slab windows' that permitted the uprise and decompression melting of
30 fertile mantle into the mantle wedge that formerly intervened between the subducted slab
31 and overlying continental crust (Hole, 1988; Hole et al., 1991, 1995; Chapter 4.1b; Fig. 2).
32 However, the relationship between the timing of no-slab window formation and the earliest
33 eruptions in each sector is not simple and there is no clear south—north age progression, a
34 feature not yet satisfactorily explained (cf. Barker et al., 1991; Hole et al., 1995). The post-
35 subduction mafic magmas consist of two sodic alkaline magmatic series characterised by
36 basanites—phonotephrites and alkali basalts—tholeiites (Smellie, 1987; Hole et al., 1995).
37 As a result, a series of extensive monogenetic volcanic fields and small isolated centres were
38 created, scattered along the length of the Antarctic Peninsula, between Seal Nunataks in the
39 north and Snow Nunataks in the south (Smellie et al., 1988; Smellie, 1999; Fig. 3). The
40 outcrops include a variety of volcanic landforms including scoria cones, tuff cones and tuyas,
41 and some outcrops are dominated by dykes. The eruptive environments varied from
42 subaerial to subglacial.

43 There have been no new field investigations of the late Neogene volcanic fields described in
44 this chapter since the detailed studies by one of us (MJH) in 1985–88. Apart from the small
45 size and isolation of the outcrops, a further major reason for the lack of study is that, in the
46 early 2000's, the Larsen A and B Ice Shelves collapsed suddenly and catastrophically, leaving
47 only a tiny relict at the nunataks, some of which are now islands. Even during the 1985–88
48 study the ambient conditions were very difficult, with wet snow and numerous large melt-
49 pools ensuring that normal over-snow travel by skidoo was difficult or impossible. Uniquely
50 in the Antarctic Peninsula, Seal Nunataks was investigated using hovercraft logistics, a
51 modus operandum that was very successful in the wet conditions. Access there now would
52 involve intensive dedicated support from helicopters.

53 Stratigraphy of the volcanic outcrops

54 A lithostratigraphy for the post-subduction alkaline volcanic outcrops in the Antarctic
55 Peninsula was published by Smellie (1999) and is broadly followed here, but with significant
56 modification. Because the outcrops are composed of laterally discontinuous volcanic rocks
57 erupted from multiple small volcanic centres, they do not easily fit with the rules of formal
58 lithostratigraphy. A simplified revised system is proposed here based on delineating volcanic
59 fields rather than formations. The new stratigraphy broadly mirrors that used in Antarctica
60 for Neogene alkaline volcanic outcrops in Victoria Land (i.e. the McMurdo Volcanic Group;
61 e.g. Kyle (1990), where geographically-delineated outcrops have been grouped within
62 volcanic provinces, each containing several volcanic fields (Chapter 5.1a). Table 1 outlines
63 the stratigraphy used here, comprising two volcanic groups (the lithostratigraphical

64 equivalent of volcanic provinces): the Bellingshausen Sea Volcanic Group and the James
65 Ross Island Volcanic Group; both groups contain multiple volcanic fields.

66 Most of the Antarctic Peninsula Neogene alkaline volcanic outcrops are described in this
67 chapter; only the Mt Haddington Volcanic Field of the James Ross Island Volcanic Group is
68 described elsewhere (Chapter 3.2a). The outcrops are mainly contained in the
69 Bellingshausen Sea Volcanic Group. However, outcrops in the Seal Nunataks Volcanic Field,
70 are conventionally regarded as part of the James Ross Island Volcanic Group (Fleet, 1968;
71 Nelson, 1975; Smellie, 1999). The Seal Nunataks Volcanic Field is geographically much closer
72 to the James Ross Island Volcanic Group compared with outcrops of the Bellingshausen Sea
73 Volcanic Group, which are c. 500 km distant (Fig. 3). However, in common with outcrops in
74 the Bellingshausen Volcanic Group, magmas in the Seal Nunataks Volcanic Province
75 probably formed as a result of decompression melting of mantle rising within no-slab
76 windows. By contrast, James Ross Island Volcanic Group magmas erupted in a back-arc
77 position coeval with subduction at the South Shetland Trench and unrelated to a no-slab
78 window (Hole et al., 1995; see Chapters 3.2a and 3.2b). Despite the contrast in tectonic
79 setting, the late Neogene volcanism throughout the Antarctic Peninsula is compositionally
80 indistinguishable and the lithofacies and eruptive palaeoenvironments are broadly similar
81 (cf. Chapter 3.2a). Although there may be a case based on tectonic setting and
82 magmagenesis to move the Sea Nunataks Volcanic Field into the Bellingshausen Volcanic
83 Group, at present we retain the distinction.

84 The outcrops described in this chapter comprise, from north to south: Seal Nunataks, Argo
85 Point, Rothschild Island, Mt Pinafore, Beethoven Peninsula, Snow Nunataks—Rydberg
86 Peninsula—Sims Island, and Merrick Mountains (Fig. 3). An additional alkaline volcanic
87 outcrop previously included consists of several lamprophyre (camptonite) dykes at Venus
88 Glacier, eastern Alexander Island (Horne and Thomson, 1967) for which a mid-Miocene age
89 of c. 15 Ma has been published (by K-Ar; Rex, 1970). However, unlike other alkaline volcanic
90 occurrences the dykes are highly altered and the isotopic age may be substantially in error.
91 Moreover, although alkaline in composition, the Venus Glacier dykes are highly altered,
92 distinctively potassic and relatively evolved (trachybasalt and phonotephrite) with
93 extraordinarily high Sr contents (Rowley and Smellie, 1990) and their genesis and affinities
94 to the post-subduction volcanism are highly uncertain. They are therefore excluded from
95 further discussion here. Other potential outcrops consist of isolated dykes with alkaline
96 compositions (e.g. in the Seward Mountains (Palmer Land) and on Adelaide Island: Smellie,
97 1987) but alkaline dykes are also known to occur in small quantity scattered across the
98 Antarctic Peninsula and, as they appear to be related genetically to the Cretaceous—
99 Tertiary arc terrain (Scarrow et al., 1998), they also do not form part of the post-subduction
100 volcanism discussed in this chapter.

101 **James Ross Island Volcanic Group**

102 *Seal Nunataks Volcanic Field*

103 Seal Nunataks is a small cluster of sixteen isolated nunataks and islands situated on the east
104 coast of northern Antarctic Peninsula (Figs 4, 5). Collectively called Seal Islands originally by

105 their discoverer, C.A. Larsen, in 1893, some of the nunataks subsequently became islands
106 following the collapse of the Larsen A ice shelf in 2000 (Pudsey and Evans, 2001). Larsen
107 (1894) described eruptions taking place during his visit to Christensen Nunatak and
108 Lindenberg Island, comprising 'funnel-like holes' (fumaroles?) emitting 'very black and thick
109 smoke'. In addition, from observations taken in 1982, González-Ferrán (1983) attributed
110 black and red tephra strewn on the ice shelf surrounding Murdoch Nunatak to recent
111 eruptive activity and he also recorded fumaroles at Dallmann and Murdoch nunataks.
112 However, although the observations by Larsen are inexplicable, the other accounts are liable
113 to doubt. A visit by one of the authors (MJH) in January 1988 showed no evidence for
114 fumaroles and there are no primary landforms. Therefore, the volcanic field at Seal
115 Nunataks is either inactive or extinct (Smellie, 1990, 1999). Conversely, the very young
116 isotopic ages (< 0.1 Ma; Table 2) obtained at several of the outcrops suggests that eruptions
117 might resume, although all the published ages are by the K-Ar method, are now quite old
118 and they should be repeated.

119 The geology of Seal Nunataks has been described by Fleet (1968), del Valle et al. (1983),
120 González-Ferrán (1983a), Hole (1990a), Smellie (1990) and Smellie and Hole (1997) and of
121 Argo Point by Saunders (1982). Published isotopic ages range between c. 4 and 0.1 Ma (Fig.
122 4; Table 2). Taken at face value, the ages suggest three broad eruptive episodes: c. 3 Ma, c.
123 1.4-1.5 Ma, and < 0.2 Ma. González-Ferrán (1983b) suggested that the ages are broadly
124 symmetrical and become younger in both directions away from a central axis but the
125 pattern is not well defined. Moreover, the ages were all obtained by the K-Ar method and
126 have high errors (typically 0.3-0.5 Ma; del Valle et al., 1983). They should be regarded simply
127 as indicative and the group would benefit substantially from more comprehensive and more
128 precise dating. Seal Nunataks dyke orientations are more variable than implied by González-
129 Ferrán (1983b). They may describe a broad arcuate pattern that is concave to the north or
130 else they are a result of intrusion along a reticulate system of fractures caused by extension
131 and rifting (Smellie, 1990; Fig. 4). The nunataks are almost all associated with prominent
132 magnetic anomalies associated with pillow lava but also interpreted to reflect deeper pipe-
133 shaped feeders extending to several kilometres rather than fissure-fed dykes (Renner,
134 1980).

135 The Christensen Nunatak Formation defined by Smellie (1999) was described as mainly
136 subaerially erupted lavas, lapilli tuffs and minor spatter, whilst the Bruce Nunatak Formation
137 was described as some combination of large dykes, pillow lava and subaqueously deposited
138 lapilli tuffs. The distinction was essentially based on eruptive setting, corresponding to
139 either subaerial lithofacies (Christensen Nunatak Formation) or subaqueous lithofacies
140 (Bruce Nunatak Formation). However, unlike the many laterally extensive eruptive units
141 (mainly lava-fed deltas) in the James Ross Island Volcanic Group (Smellie et al., 2013;
142 Chapter 3.2a), situated < 150 km to the northeast of Seal Nunataks and overlapping in age,
143 Seal Nunataks is formed of multiple small eruptive centres with a very localised distribution
144 of the erupted products and no meaningful stratigraphical correlations can be made
145 between the centres. There are no known outcrops of lava-fed deltas in the Seal Nunataks
146 Volcanic Field. By contrast, the geographically separate outcrop at Argo Point is distinctive
147 within the volcanic field: it is a well-formed scoria cone.

148 The principal characteristics of the individual outcrops are now briefly described (see Fig. 4).

149 **Åkerlundh Nunatak:** This is the smallest of the Seal Nunataks, just 90 m high. It forms an
150 elongate ridge formed around a central 25 m-wide dyke of vesicular olivine-plagioclase-
151 phyric basalt with an age of 0.7 ± 0.3 Ma (del Valle et al., 1983). There are also rare isolated
152 and small outcrops of vesicular plagioclase-phyric pillow lava and poorly bedded black
153 lapillistone.

154 **Arctowski Nunatak:** This nunatak rises c. 235 m above the Larsen Ice Shelf and it comprises
155 a 50-70 m-wide dyke zone orientated $285^\circ N_{mag}$ composed of olivine-plagioclase-phyric
156 basalt. The dyke margins are locally bulbous and there are internal chilled margins
157 suggesting that the dyke is multiple, together with three small (c. 35 cm wide) dykes aligned
158 at c. $340^\circ N_{mag}$. Pillow lava with distinctive acicular aggregates of plagioclase phenocrysts is
159 well exposed on the eastern flank of the nunatak. A dyke dated by del Valle et al. (1983)
160 yielded an age of 1.4 ± 0.3 Ma.

161 **Bruce Nunatak:** Bruce Nunatak comprises three ridges rising to 320 m asl constructed
162 around multiple dykes trending 270 , 010 and $221^\circ N_{mag}$. Olivine-plagioclase-phyric pillow lava
163 is conspicuous particularly on the flanks of the ridges, the northern slopes and in the centre.
164 Yellow-orange lapilli tuffs with scattered lava blocks up to 15 cm long and laminated tuffs
165 are exposed in the northern face of the nunatak. The pyroclastic rocks are extensively
166 affected by syndepositional faulting and slumping, including local zones of chaotic blocks in
167 lapilli tuff matrix (Fig. 5f). Prominent slump planes dip at 23° to the west-northwest. A dyke
168 dated by del Valle et al. (1983) yielded an age of 1.5 ± 0.5 Ma.

169 **Bull Nunatak:** This is a conical-shaped nunatak that rises c. 175 m above the Larsen Ice
170 Shelf. It is composed of at least two generations of north—south and east—west-trending
171 olivine-phyric dykes but the majority of the nunatak consists of lava, with pillows up to 1.5
172 m in diameter. Olivine-phyric agglutinate overlying the lava is exposed locally on the
173 northwest side. The lava pillows are slightly to moderately flattened and lack interpillow
174 debris, features that may be more consistent with subaerial pāhoehoe, but distinction is
175 uncertain.

176 **Castor Nunatak:** This nunatak, rising to c. 155 m above the Larsen Ice Shelf, comprises a
177 snow dome that caps a near-horizontal sequence of lavas and pyroclastic rocks; dykes are
178 absent. The nunatak may preserve a lava-filled crater (Smellie and Hole, 1997). The lavas are
179 'a'ā with bright red oxidised clinkery to locally ropy surfaces. They are locally interbedded
180 with, but mainly overlie, subhorizontally bedded yellow-orange lapilli tuffs with accretionary
181 lapilli, a few thin tuff and some breccias in which large channel-like structures are common
182 and conspicuous (Fig. 5e).

183 **Christensen Nunatak:** The summit of this nunatak is at c. 300 m asl and it consists of a 20 m-
184 thick lower horizontal columnar jointed lava overlain by c. 50 m of yellow-orange pyroclastic
185 rocks and then an upper thin (< 3 m) lava. Both lavas have oxidised vesicular upper surfaces
186 and are olivine phyric. The pyroclastic rocks are yellow-orange lapilli tuffs, well bedded and
187 with scattered lava blocks, some with impact structures. There are also a few thin dykes

188 lacking an overall orientation that cut the pyroclastic deposit. There is a published isotopic
189 age of 0.7 ± 0.3 Ma (del Valle et al., 1983).

190 **Dallmann Nunatak:** This nunatak is c. 210 m high and is broadly conical overall (Fig. 5a). A
191 crater that issued a fresh-looking lava flow were sketched and described by González-Ferrán
192 (1983a) but neither feature appears to exist. Exposure is very poor and seems to comprise
193 only lava with poorly defined pillow-like structures (Fig. 5c). Although they may indicate
194 pāhoehoe rather than pillow lava, interpretation is equivocal (as on Bull Nunatak, above).

195 **Donald Nunatak:** A small nunatak that rises c. 100 m above the Larsen Ice Shelf, this
196 outcrop has pyroclastic rocks exposed at its western end. It has a published K-Ar age of < 0.2
197 Ma (del Valle et al., 1983). The pyroclastic rocks comprise horizontally bedded yellow-
198 orange and dark grey lapilli tuffs or lapillistones, tuffs and breccias with numerous flattened
199 bombs, the latter also occurring as weakly agglutinated layers up to 15 cm thick. The yellow-
200 orange and dark grey deposits are in subvertical contact with no obvious structural break,
201 suggesting that the yellow coloration is an alteration artefact. A single dyke trending
202 $360^\circ N_{mag}$ cuts the pyroclastic rocks and is locally brecciated, with mingling of the dyke
203 fragments and yellow lapilli tuff or lapillistone.

204 **Evensen Nunatak:** This nunatak is a ridge formed by a grey vesicular olivine-phyric dyke that
205 rises c. 160 m above the Larsen Ice Shelf and is c. 1 km in length. It has K-Ar ages of 1.4 ± 0.3
206 and 4.0 ± 1 Ma (del Valle et al., 1983). The dyke zone is c. 50 m wide and has multiple chilled
207 surfaces hence is multiple. Small exposures of black vesicular plagioclase-phyric basalt lava
208 commonly with ropy surfaces are present near the nunatak summit and on the north flank.

209 **Gray Nunatak:** Gray Nunatak is < 2 km long and rises c. 100 m above the Larsen Ice Shelf. It
210 consists of four east—west-trending en echelon ridges, each formed around a dyke. The
211 rock has a published age of < 0.2 Ma (del Valle et al., 1983). The dykes are olivine-
212 plagioclase-phyric and have trends varying between 233 and $281^\circ N_{mag}$. There are also rare
213 exposures of pillow lava poorly seen in the scree-covered flanks and, from the abundance of
214 pillow lava debris it is likely that the nunatak is dominated by pillow lava. A sill-like outcrop
215 of basalt with conspicuous olivine and plagioclase phenocrysts up to 1 cm long is also
216 present in the southwest. Finally, a few very small exposures of yellow-orange lapilli tuff are
217 also present close to the dyke zone.

218 **Hertha Nunatak:** This is a small nunatak but it rises c. 225 m above the Larsen Ice Shelf. It is
219 largely snow covered but its elongate nature suggests that it may have formed around an
220 (unexposed) east—west-trending dyke. A conical hill at the western end is formed of five
221 horizontal olivine-plagioclase-phyric lavas individually up to 7 m thick and with prominent
222 oxidised ropy surfaces. Apart from rare loose blocks of brownish-black lapillistone or lapilli
223 tuff and breccia, no other lithologies are present.

224 **Larsen Nunatak:** Larsen Nunatak is a single ridge < 2 km long that rises c. 140 m above the
225 Larsen Ice Shelf and centred around a poorly exposed, east—west-trending olivine-
226 plagioclase-phyric dyke zone (Fig. 5d). It has a K-Ar age of 1.5 ± 0.5 Ma (del Valle et al.,
227 1983). The ridge flanks are extensively covered by lava pillows up to 1 m long.

228 **Lindenberg Island:** Rising c. 200 m above its surroundings, this nunatak is an east—west-
229 trending ($270^{\circ}\text{N}_{\text{mag}}$) ridge formed by an olivine-plagioclase-phyric dyke. There are also rare
230 exposures of yellow-orange lapilli tuff, tuff and breccia at the west end of the ridge.

231 **Murdoch Nunatak:** This is the largest nunatak in the group but it is mostly covered by scree.
232 It is c. 370 m high (c. 320 m above the Larsen Ice Shelf) and has an area of c. 4 km², with a
233 flat top and steep sides. A central zone of multiple dykes trends c. $320^{\circ}\text{N}_{\text{mag}}$ and other
234 thinner dykes trend $325^{\circ}\text{N}_{\text{mag}}$. Olivine-plagioclase-phyric pillow lava is well exposed on the
235 west side and summit ridge and there is a series of small exposures of black agglutinate with
236 ropy textures on the north side. Lava bombs litter the surface of the nunatak. Near the
237 summit there are small occurrences of yellow-orange lapilli tuff and tuff and dark grey to
238 buff-coloured lapillistones containing fluidal bombs.

239 **Oceana Nunatak:** This is the only volcanic outcrop on Robertson Island (formed of Late
240 Jurassic sedimentary rocks; [Riley et al., 1997](#)). It rises to 270 m a.s.l. and consists of an
241 olivine-plagioclase-phyric dyke core (two sets, trending $250\text{--}260^{\circ}\text{N}_{\text{mag}}$ (main dyke zone) and
242 $348\text{--}010^{\circ}\text{N}_{\text{mag}}$). Pyroclastic rocks crop out in a 10 m-high crag at the east end, comprising
243 poorly bedded, massive brownish-grey lapillistone with scattered flattened olivine-phyric
244 bombs. At the west end is a well-bedded association of yellow-orange tuff, lapilli tuff and
245 tuff breccia with rare lava pillows. The western outcrop is also crossed by numerous small-
246 displacement faults reflecting slumping directed towards the northwest. A dyke dated by [del](#)
247 [Valle et al. \(1983\)](#) yielded an age of 2.8 ± 0.5 Ma.

248 **Pollux Nunatak:** There is no exposure on this tiny nunatak, which is entirely formed of scree
249 composed of likely dyke fragments.

250 **Argo Point:** This locality is situated on the east coast of Jason Peninsula, c. 140 km south of
251 Seal Nunataks ([Fig. 3](#)). It consists of a small basaltic scoria mound measuring c. 300 m in
252 diameter that is breached on its northern side. The mound has numerous bombs and blocks
253 on its surface and it is associated with a prominent trail of debris extending in a
254 northeasterly direction on the adjacent heavily crevassed ice shelf ([Fig. 6](#)). The debris trail is
255 today > 4 km long ([Saunders, 1982](#), estimated > 1 km) and is formed of basalt lava and
256 scoria. It was described by [Saunders \(1982\)](#) as a moraine created by active ice erosion but it
257 also possible that at least some of the debris is a wind tail caused by a combination of strong
258 local winds redistributing loose materials of the scoria cone, followed by northeasterly flow
259 of the ice shelf, as has been observed for similar deposits at Seal Nunataks ([González-Ferrán,](#)
260 [1983a](#)). Inaccessible cliffs beneath the scoria mound comprise olivine-plagioclase-phyric
261 basalt lavas with ropy textures and scoria ([Saunders, 1982](#)). The scoria mound has published
262 ages of 0.8 ± 0.1 and 1.0 ± 0.3 ([Smellie et al., 1988](#)).

263 Finally, an isolated outcrop situated on the south side of Jason Peninsula c. 37 km west of
264 Argo Point also yielded very young K-Ar ages of 1.3 ± 0.3 and 1.6 ± 0.5 Ma ([Smellie et al.,](#)
265 [1988](#)). However, that outcrop is a hematite-coated intrusion, implying that it is relatively
266 altered, and its composition is tholeiitic, poor in alkalis and low in Nb. It thus more closely
267 resembles the Mesozoic volcanic outcrops that dominate the geology of Jason Peninsula
268 and are probably related to extension caused by the migration of a giant plume head

269 associated with Gondwana break-up and which triggered widespread bimodal mostly
270 explosive volcanism in the Antarctic Peninsula (Saunders, 1982; Smellie, 1991; Riley et al.,
271 2010; Pankhurst et al., 2000; Riley and Leat, this volume (Chapter 2.2a)). It therefore does
272 not belong to the very young post-subduction volcanism and its apparently very young age
273 is currently unexplained.

274 **Bellingshausen Sea Volcanic Group**

275 The Bellingshausen Sea Volcanic group encompasses widely scattered isolated outcrops in
276 Alexander Island and Palmer Land (Fig. 3). They comprise: (1) Rothschild Island; (2)
277 Alexander Island (Mt Pinafore and Debussy Heights; Beethoven Peninsula); (2) Palmer Land
278 (Henry Nunataks, Merrick Mountains; Sims Island; Rydberg Peninsula; Snow Nunataks; Fig.
279 7). The outcrops were first discovered by Bell (1973) with additional outcrops discovered
280 and described by Care (1980), Burn and Thomson (1981), Laudon (1982) and O'Neill and
281 Thomson (1985). All are small and those situated on the flanks of Mt Pinafore (northern
282 Alexander Island) are on high ridges with difficult access (Figs 8a,b). In addition, Snow
283 Nunataks and outcrops in the Merrick Mountains are remote and have been visited only
284 once (Thomson and Kellogg, 1990; Rowley et al., 1990; Thomson and O'Neill, 1990). As a
285 result, with a few exceptions (Smellie et al., 1993; Smellie and Hole, 1997), most outcrops
286 have been studied only at reconnaissance level.

287 *Mt Pinafore Volcanic Field*

288 **Rothschild Island** is a large island situated off the northwest coast of Alexander Island. It
289 contains two small volcanic outcrops at its southeastern end close to Overton Peak (Care,
290 1980; Overton Peak Formation of Smellie, 1999). No contacts with bedrock are exposed and
291 the outcrops may be fault controlled. The southwestern outcrop is a cliff 100 m high. The
292 basal 25 m of the section there comprises irregularly bedded pale yellow and brown tuffs
293 and lapillistones showing crude polygonal jointing. Beds are commonly 2-10 cm thick, but
294 vary up to c. 1 m. Cross lamination is present. The overlying section is composed of > 30 m
295 of dark and pale grey lapilli tuffs in beds variably 2-30 cm thick, often normally graded, and
296 with lapillistones and tuffs towards the top. The northeastern outcrops consist of two small
297 rounded hills, which are dominated by basaltic scree including black scoriaceous clinkers;
298 there are also rare exposures of lapilli tuff and tuff similar to the southwestern outcrop
299 described above. Beds are up to 35 cm thick and they show abundant cross lamination and
300 channels consistent with subaqueous deposition, and small-scale faulting. Both of the
301 principal outcrops are intruded by dykes that form a multiple dyke zone 50 m wide with
302 narrow screens of lapilli tuff and tuff in the northeastern outcrop, from which a K-Ar isotopic
303 age of 5.4 ± 0.8 Ma was obtained (Smellie et al, 1988). The two principal outcrop areas are
304 separated by 6 km and they may have been formed by eruptions from two separate small
305 tuff cone centres, an origin that is different to other outcrops in the Mt Pinafore Volcanic
306 Field (see below).

307 **Alexander Island:** Mt Pinafore in the Elgar Uplands region of northern Alexander Island
308 includes three localities on Mt Pinafore itself, another situated near Ravel Peak (Debussy
309 Heights) c. 15 km southwest of the other outcrops, and one at Hornpipe Heights c. 10 km to

310 the south-southwest (Burn and Thomson, 1981; Hole and Thomson, 1990; Hole, 1990b; Fig.
311 7). There are two types of outcrop based on the dominant lithofacies, which were used as
312 the basis for separation into two stratigraphical units (formations) by Smellie (1999): the Mt
313 Pinafore Formation, comprising the three outcrops at Mt Pinafore and that at Ravel Peak;
314 and the Hornpipe Heights Formation, at Hornpipe Heights only (Fig. 9). An additional locality
315 c. 13 km northeast of Mt Pinafore was shown as a volcanic outcrop of similar age on the
316 map by Hole and Thomson (1990) but was not described. It consists of a plug-like mass c. 30
317 m in diameter and 100 m high formed of massive polymict tuff breccia with numerous
318 blocks of MeMay Group metasediments, Tertiary volcanics and spheroidally-weathered
319 dolerite up to 1 m across in a basaltic tuff matrix. The outcrop is capped by a layer of brown
320 well-bedded similarly-polymict lapilli tuff, and a fresh-looking olivine dolerite crops out
321 locally at the plug margin and is associated with several thin basaltic dykes. Although it is
322 undated, the locally pervasive deuteric alteration of the outcrop and a likely calc-alkaline
323 composition (based on petrographical characteristics) suggest that the outcrop is not Mio-
324 Pliocene but is probably a vent-fill and part of the compositionally distinctive Early Tertiary
325 subduction-related volcanism that is widespread in Elgar Uplands nearby (Burn, 1981;
326 McCarron, 1997; McCarron and Millar, 1997; McCarron and Smellie, 1998; Chapter 3.1b).

327 The four constituent outcrops at **Mount Pinafore and Debussy Heights** occupy
328 palaeovalleys cut in bedrock (deformed metasedimentary strata of the LeMay Group; Burn,
329 1984). The lithofacies can be grouped into two principal associations, a basal epiclastic—
330 volcanoclastic association of volcanic sandstone and conglomerate, and an upper
331 volcanogenic association of lava and hyaloclastite breccia or tuff breccia (Figs 8, 9; Hole and
332 Thomson, 1990; Smellie et al., 1993; Smellie and Skilling, 1994). Outcrop thicknesses vary
333 from 60 to > 80 m. The basal association consists of some combination of beds and lenses of
334 massive polymict pale grey sandy conglomerate with abundant abraded nonvolcanic (local
335 basement) clasts up to 75 cm across; polymict sandy volcanic pebble conglomerate with
336 crude wavy planar stratification; multistorey beds of polymict gravelly volcanic sandstone
337 with planar and cross stratification commonly associated with broad shallow channels up to
338 3 m across; and flaggy monomict fine volcanic sandstone or lapilli tuff and tuff. Some of the
339 underlying basement surfaces locally show signs of glacial modification (striations, ice
340 moulding) and the overlying nonvolcanic conglomerates contain rare striated and faceted
341 clasts. The associated sediments are generally yellow-brown in colour due to palagonite
342 alteration of sideromelane. They were sourced in contemporary volcanic materials, mainly
343 sideromelane reworked from unconsolidated lapilli and ash. The blocky variably vesicular
344 sideromelane fragments and abundant ash suggest a phreatomagmatic origin for the
345 volcanism. Because the volcanic-derived deposits are first-cycle sediments, they might also
346 be given primary volcanic names (lapilli tuffs and tuffs; White and Houghton, 2006) although
347 the enclosed pebbles are often well rounded. The overlying volcanic lithofacies association
348 is dominated by thick basaltic sheet lavas often showing spectacular columnar jointing
349 (mainly entablature with much thinner basal and rare upper colonnades). Some examples
350 comprise valley-confined (pooled) single lavas up to c. 80 m thick. The lavas may have
351 pillowed and brecciated lava margins that are in intimate contact with yellow-orange
352 hyaloclastite and tuff breccia. The latter are massive to crudely and coarsely stratified, and

353 formed of blocky mainly poorly to nonvesicular sideromelane. Two of the outcrops show
354 only a single pair of lithofacies associations consistent with single eruptive events, whereas
355 two others, including that at Ravel Peak, appear to have two or more pairs of associations.
356 Numerous K-Ar ages have been determined on all four outcrops and vary between 7.7 ± 0.6
357 and 3.9 ± 0.4 Ma (Smellie et al., 1988). It is likely that the youngest age is spurious and the
358 five eruptive episodes are dated as c. 7.6, 7.0, 6.1 (2 different localities) and 5.4 Ma.

359 The **Hornpipe Heights** outcrop is spectacular and has been thoroughly studied (Hole, 1990b,
360 and unpublished; Smellie, 1999). The mainly red-coloured (oxidised) lithofacies drape and
361 infill cracks and gullies on the steep north-facing flank of a ridge composed of local non-
362 volcanic basement rocks (LeMay Group metasediments; Figs 9, 10). The sequence extends
363 up a few hundred metres, almost the full height of the ridge, but it is just c. 20 m in
364 thickness and has a general dip of c. 40° , with some beds dipping up to 52° . Close to the
365 base of the sequence, a local lens of massive polymict orthobreccia is present, up to 2.5 m
366 thick and 3 m long. It is composed of abundant crudely parallel slabs and blocks of the local
367 basement (LeMay Group sandstone), together with basalt lava blocks and scoria in a
368 tuffaceous matrix. The rest of the sequence consists of lapillistones with numerous disk-like
369 (cowpat) bombs of olivine basalt. Some beds are reverse graded and erosion-like surfaces
370 are present, occasionally showing channel-like steep-sided profiles. Oxidised agglutinate
371 formed of weakly welded large aerodynamic bombs also occurs and becomes coarser up-
372 sequence. There are also yellowish, buff and red-coloured interbedded fine lapillistones and
373 tuffs, some of the latter showing asymmetrical ripple-like bedforms with amplitudes up to 5
374 cm that may be a product of slope instability together with minor syndepositional faulting.
375 The yellow discoloration affecting some beds is caused by marginal palagonite alteration of
376 sideromelane grains. Several thin (< 2 m), platy, grey, olivine- and plagioclase-olivine-phyric
377 highly vesicular lavas, some with poorly developed columnar jointing, occur mainly within
378 the upper part of the sequence; they are probably clastogenic. Others, near the base of the
379 slope, contain 'pillow-like' forms (pāhoehoe toes?). No vent for the sequence has been
380 identified. There are two published K-Ar isotopic ages: 2.5 ± 0.8 and 2.7 ± 0.2 Ma (Smellie et
381 al., 1988).

382 *Beethoven Peninsula Volcanic Field*

383 **Beethoven Peninsula** in southwestern Alexander Island contains ten largely snow-covered
384 nunataks and hills scattered over an area of c. 2500 km², of which six of the features have
385 exposed volcanic rock although all are probably volcanic in origin (Fig. 7). Only five of the
386 nunataks have been visited (Bell, 1973; Hole, 1990c; Smellie and Hole, 1997). Based on the
387 presence and distribution of strong magnetic anomalies (Renner et al., 1982), the volcanic
388 field at Beethoven Peninsula may be very extensive and it may also underlie most of
389 Monteverdi Peninsula to the southeast and Latady Island to the northwest (Fig. 3). If true,
390 the combined area of volcanic rock would exceed 7000 km², making it the largest volcanic
391 field in the Antarctic Peninsula south of James Ross Island (Smellie and Hole, 1997; Smellie,
392 1999; cf. Smellie et al., 2013). The most accessible and informative outcrop on Beethoven
393 Peninsula is that forming the larger (southwestern) of the two Mussorgsky Peaks (summit
394 elevation c. 500 m a.s.l.; Fig. 11b). The inaccessible but similarly well exposed sequence at

395 Mt Grieg (summit elevation c. 600 m a.s.l.) is also informative but has only been viewed at a
396 distance (Fig. 11a). Two lithofacies associations are present, corresponding to lava-fed delta
397 and subaqueous tuff cone lithofacies (Smellie and Hole, 1997). Subaqueous lithofacies crop
398 out at Mussorgsky Peaks, Mt Liszt and Mt Strauss and they form the thick (c. 250-300 m)
399 basal section at Mt Grieg; it is inferred that another four outcrops may be formed of similar
400 lithofacies, at Mt Tchaikovsky, Mt Lee, Mt Schumann and Chopin Hill, but they have not
401 been visited. The subaqueous lithofacies comprise yellow-orange crudely bedded lapilli tuff
402 and lesser thin-bedded tuff containing channel and dewatering structures and displaced
403 slabs of tuff up to 1 m long. Massive chaotic olivine-phyric lava pillows and pillow breccia
404 mingled with yellow lapilli tuff also underlies the volcanoclastic rocks at the eastern
405 Mussorgsky Peaks outcrop. Large and small syn-sedimentary slump structures (cf. Mt
406 Benkert, below) and faulting are also common and conspicuous. Several southwest—
407 northeast-trending olivine-plagioclase-phyric dykes cut the Mussorgsky Peaks outcrops. The
408 thickest exposed sequence of subaqueous lithofacies is c. 200 m thick, at southwestern
409 Mussorgsky Peaks although the entire sequence may be substantially thicker (up to 500 m,
410 assuming continuity of outcrop down to bedrock; Smellie, 1999). Mt Liszt and Mt Strauss are
411 composed of yellow-orange lapilli tuffs similar to the basal Mussorgsky Peaks sequence.

412 Lithofacies that form lava-fed deltas form a capping sequence up to 100-150 m thick at Mt
413 Grieg and the western Mussorgsky Peak and it may also include the sequence exposed at
414 Gluck Peak. The sequence at Mt Grieg is inaccessible but it can be studied easily using
415 binoculars. At Mussorgsky Peaks, the lithofacies comprise pillow-fragment breccia and
416 minor pillow lava that form a spectacular thick (100 m) dark grey unit showing large-scale
417 homoclinal dipping bedding that oversteps underlying yellow-orange volcanoclastic rocks
418 of the Mussorgsky Peaks Formation (Fig. 11b); although flat-topped, the summit of
419 Mussorgsky Peaks is inaccessible and it is unclear if any subaerial lavas are preserved.
420 However, lavas are preserved at Mt Grieg where they form a 50-100 m-thick capping unit of
421 horizontal grey pāhoehoe(?) lavas. Gluck Peak is formed of dark grey pillow lava and pillow
422 breccia similar to that capping Mussorgsky Peaks but with less abundant breccia. Moreover,
423 compared to the latter, the constituent lava pillows at Gluck Peak are much more highly
424 vesicular and they were fed by dykes similar to relations seen at Seal Nunataks.

425 The Beethoven Peninsula outcrops are very poorly dated. K-Ar isotopic ages of 2.5 and 0.68
426 ± 0.97 Ma were reported for samples from Mussorgsky Peaks and Gluck Peak, respectively,
427 without analytical details (Hole, 1990c). The very young age from Gluck Peak (i.e. essentially
428 undateable) suggests that the volcanic field is potentially still active but, in common with all
429 the other outcrops on Beethoven Peninsula, Gluck Peak is extensively eroded and there are
430 no primary volcanic landforms. However, thermal waveband satellite imagery of Gluck Peak
431 has revealed elevated heat flow situated on the summit of Gluck Peak, with inferred
432 temperatures well above background or locally enhanced insolation (personal
433 communication from Peter Fretwell, British Antarctic Survey, 2016). The occurrence is most
434 readily explained as enhanced geothermal (volcanic) heat. If confirmed, this would be the
435 first occurrence of geothermally heated warm ground to be discovered in the Antarctic
436 Peninsula region outside of Bransfield Strait (i.e. the Deception Island active volcano and
437 Bransfield Strait seamounts; see Chapters 3.1a and 8.1).

438 *Merrick Mountains Volcanic Field*

439 Two very poorly known, small and isolated volcanic outcrops are present at **Henry Nunataks**
440 **and Merrick Mountains** in southern Palmer Land (Fig. 7; Halpern, 1971; Rowley et al., 1990;
441 Smellie, 1999). The outcrop at Henry Nunataks (possibly two discrete outcrops, only one
442 unvisited; Thomson and Kellogg, 1990) is composed of c. 100 m of gray aphanitic basalt
443 lavas ('a'ā?) with rubbly surfaces cut by a dyke. The Merrick Mountains outcrop (west of
444 Eaton Nunatak) is extensively frost shattered but is formed of basanite lava breccia with a
445 palagonite-altered glassy matrix (possibly hyaloclastite). It is overlain by thin vesicular to
446 scoriaceous lavas (Laudon, 1982; Smellie, 1999) for which Halpern (1971) reported a K-Ar
447 age of 6 Ma. However, the age lacks published analytical details and its reliability is
448 uncertain.

449 *Snow Nunataks Volcanic Field*

450 Several volcanic outcrops occur in the Rydberg Peninsula—Sims Island—Snow Nunataks
451 area of southwestern Palmer Land (Renner et al., 1982; O'Neill and Thomson, 1985; Rowley
452 and Thomson, 1990; Thomson and O'Neill, 1990; Hathway, 2001; Fig. 7). Those at **Rydberg**
453 **Peninsula** may include the several hundred metres-high and 3.5 km wide cone-shaped
454 Mount Combs but it is completely snow covered. However, a small exposure of undated
455 subaerial olivine-phyric basalt lavas occurs c. 15 km northeast of Mount Combs (Renner et
456 al., 1982, and unpublished field notes of R.G.B. Renner, 1976). **Sims Island** is a prominent
457 feature 3 km in length that rises to c. 380 m a.s.l. It is constructed of basal olivine basalt
458 pillow lava overlain by 30–40 m of thick-bedded pillow breccia and 'gravelly volcanic
459 sandstone' (probably lapilli tuff) then more pillow lava that forms the remainder of the pile
460 (Fig. 12). Inaccessible bedded clastic deposits may cap the sequence and large irregular
461 columnar intrusions are present and especially prominent to base. The Sims Island sequence
462 has published $^{40}\text{Ar}/^{39}\text{Ar}$ ages of 3.46 ± 1.20 and 2.30 ± 0.54 Ma, of which the latter (with
463 lower errors) is regarded as more reliable (Hathway, 2001).

464 **Snow Nunataks** are an east—west-trending chain of four volcanic outcrops (O'Neill and
465 Thomson, 1985; Thomson and O'Neill, 1990). Similar to Beethoven Peninsula outcrops, two
466 lithofacies associations have been defined based on differing lithofacies characteristics
467 (Smellie, 1999). Subaqueously erupted and emplaced basalt pillow lava and orange-brown
468 lapilli tuff crop out at Mt Benkert and Mt Thornton and form the basal sequence of Mt
469 McCann. They also form the Sims Island outcrop (c. 30 km to the northwest; Figs 7, 12). The
470 proportions of the two main lithofacies vary: pillow lava is 200 m thick at Mt McCann and is
471 capped by just 5 m of lapilli tuff whereas spectacular exposure at Mt Benkert is formed of at
472 least 350 m of lapilli tuff with minor pillow lava, pillow breccia and thin massive lavas (Fig.
473 13). The latter also show channel structures on a range of scales, including spectacular
474 channels a few hundred metres wide and up to 50 m deep that are probably the two-
475 dimensional traces of slump scars (cf. Smellie, 2018). The Mt Thornton sequence is similar to
476 that at Mt Benkert in that it is dominated by massive and thin-bedded lapilli tuffs that show
477 much evidence for slope instability (convolute layering and folding), but it also has poorly
478 exposed pillow lava and blocky lava (lava breccia?) at its base. Subaerially erupted
479 scoriaceous and clinkery basalt rubble and massive vesicular lavas form the upper sequence

480 at Mt McCann, whilst Espenchied Nunatak is formed of crudely stratified black and reddish-
481 brown lapilli tuff and tuff breccia intruded by very thin (3 cm) basalt dykes. Isotopic ages (all
482 by K-Ar) range between 20 and 1.6 Ma (unpublished information of JW Thomson, cited by
483 [Smellie et al., 2009](#)). There are no published analytical details and the oldest age (from Mt
484 McCann) may be unreliable, but Mt Benkert is c. 4.6 Ma and Mt Thornton is c. 1.6 Ma ([Table](#)
485 [2](#)).

486 **Physical volcanology and palaeoenvironmental inferences**

487 Apart from generally small isolated outcrops of subaerial lavas or scoria cones (at Argo
488 Point, Hornpipe Heights, Henry Nunataks and Rydberg Peninsula), the Antarctic Peninsula
489 post-subduction volcanism appears to have been overwhelmingly glaciovolcanic, i.e.
490 erupted in association with an ice sheet ([Smellie et al., 1988, 1993](#); [Smellie and Skilling,](#)
491 [1994](#); [Smellie and Hole, 1997](#)). Investigations of the outcrops have been used to reconstruct
492 multiple critical parameters of the mainly Mio-Pliocene Antarctic Peninsula Ice Sheet by
493 [Smellie et al. \(2009\)](#). The Antarctic Peninsula (south of James Ross Island; see Chapter 3.2a)
494 contains two principal generic types of glaciovolcanic outcrops corresponding to sheet-like
495 sequences and tuyas ([Smellie and Edwards, 2016](#)). Sheet-like sequences are defined by their
496 association of water-chilled sheet lava and waterlain volcanoclastic deposits that have a
497 laterally extensive sheet- or ribbon-like geometry. The absence of internal erosional or
498 otherwise time-significant unconformities indicates that the two associations form a
499 genetically related multistorey unit constructed during a single eruptive event. Two types
500 have been defined: the Mt Pinafore type, with the Alexander Island occurrences given the
501 status of sequence holotypes by [Smellie and Skilling \(1994](#); also [Smellie et al., 1993](#)), and the
502 Dalsheidi type, based on outcrops in southern Iceland ([Smellie, 2008](#)). However, it now
503 seems likely that the two 'types' previously recognised are simply variants occurring in a
504 broad continuum of deposits ([Smellie and Edwards, 2016](#)). Tuyas are the most distinctive
505 morphological expression of glaciovolcanism, characterised by a flat or gently domed top
506 and steep sides ([Mathews, 1947](#); [Smellie, 2013](#); [Smellie and Edwards, 2016](#)). The flat or
507 gently domical top is an expression of the construction of a small subaerial shield whereas
508 the steep flanks are a primary feature formed as a result of the lateral progression of one or
509 more lava-fed deltas, in which the subaerial capping lavas (analogous to delta topset beds)
510 overlie homoclinal, steep-dipping foreset beds of breccia and tuff breccia (formerly called
511 hyaloclastite; see discussion in [Smellie and Edwards, 2016, pp. 197-205](#)). The prominent
512 planar structural discontinuity that separates the lavas from tuff breccia is called a passage
513 zone and it is a fossil water level. It represents the migrating position of the delta brink point
514 at which the subaerial lava is rapidly cooled by water and mechanically broken, with the
515 glassy and aphanitic lava fragments tumbling down the delta front together with larger scale
516 delta front collapses ([Skilling, 2002](#); [Smellie and Hole, 1997](#)).

517 The sheet-like sequences are confined to northern Alexander Island, i.e. at Mt Pinafore and
518 Ravel Peak. In general, the basal parts of the sequences are composed of fragmental rocks
519 transported and deposited by flowing water. A wet-based glacial (sub-ice) eruptive setting
520 was inferred because of the following observations: (i) the underlying bedrock surface is
521 commonly striated or otherwise ice-moulded and may be overlain by polymict diamict

522 interpreted as till (possibly flow or meltout till); (ii) the associated lavas are very fine grained
523 (aphanitic) indicating rapid chilling; and (iii) the prismatic to hackly (blocky) jointing and rare
524 presence of pillow lava are characteristic of abundant water and associated strong cooling
525 (Smellie and Hole, 1997; also Smellie and Edwards, 2016, pp. 193-197). Some of the lavas
526 are very thick (up to 80 m) suggesting that they were ponded either in a topographical
527 depression or else by a barrier of coeval ice if the lavas flowing beneath thinner ice in a
528 tributary valley abutted much thicker ice in a major trunk glacier (cf. Lescinsky and Sisson,
529 1998). The basal fragmental beds are mainly traction current deposits laid down under
530 variable flow states, including upper flow regime conditions. In view of the valley-confined
531 setting and by analogy with the study of a broadly comparable sequence in Iceland by
532 Walker and Blake (1966), formation within a confined ice tunnel was inferred by Smellie et
533 al. (1993). The thickness of tabular cross stratified units present (typically 40-60 cm) is
534 qualitatively consistent with flow depths of c. 1-5 m and analogy was made with esker
535 deposits in non-volcanic glacial systems (Smellie and Skilling, 1994; but see Smellie and
536 Edwards, 2016, pp. 176). Although some of the epiclastic deposits are polymict, most are
537 monomict and formed of reworked and redeposited sideromelane whose blocky shapes and
538 variable vesicularity suggest derivation in unconsolidated phreatomagmatic tephra,
539 probably a tuff cone constructed at an early stage of the glaciovolcanic event. The overlying
540 volcanic lithofacies (sheet lava, locally pillowed, and tuff breccia) indicate strong water
541 chilling and it seems likely that the entire sequence was at least intermittently flooded by
542 water during its formation. Although minor hyaloclastite (sensu White and Houghton, 2006)
543 may be present locally, where lava was chilled and fragmented in situ in water and against
544 wet tuff breccia, the host volcanoclastic deposit is typically relatively fine grained (lapilli tuff)
545 and shows crude coarse planar stratification characteristic of deposition mainly from
546 hyperconcentrated density flows during subglacial meltwater flood events (Loughlin, 2002;
547 Smellie, 2008) which, in the Alexander Island examples, were probably tunnel-confined
548 (Smellie et al., 1993). Because the lithofacies in most sheet-like sequences are subaqueous,
549 they only provide a crude minimum estimate for the thickness of coeval ice. Although the
550 associated ice is generally thought to have been relatively thin (\leq c. 150 m; Smellie, 2000 
551 consistent with the thinness of the sequences (tens of metres), there are normally no
552 cogenetic subaerial lithofacies that might give a clue to the elevation of the original ice
553 surface.

554 Most of the other volcanic outcrops represent tuyas in various stages of construction. They
555 make up multiple centres in the Seal Nunataks, southeastern Rothschild Island, Beethoven
556 Peninsula and Snow Nunataks volcanic fields. Those outcrops in the Seal Nunataks and
557 Beethoven Peninsula volcanic fields show different stages in the evolution of tuyas caused by
558 varying coeval ice thicknesses. They were used to illustrate the varied lithofacies and
559 lithofacies architectures in tuyas and to erect a general model for tuya construction (Fig. 14;
560 Smellie and Hole, 1997). The outcrops occur in isolation and a glacial setting for the tuya
561 volcanism was inferred mainly because the subaqueous sequences are several hundred
562 metres thick, implying a similar high coeval water elevation and thus ponding by ice.
563 Moreover, there is no palaeotopography with which a non-glacial (pluvial) lake might have
564 been confined and the elevations of the subaqueous lithofacies are generally too high to be

565 explained by marine construction followed by major regional uplift. Relationships between
566 some of the lithofacies associations are also irreconcilable with a marine setting (see below).
567 The best exposed examples are at Mussorgsky Peaks and (inaccessible) Mt Grieg on
568 Beethoven Peninsula (Alexander Island), which show the prominent bipartite division into
569 two distinctive lithofacies associations typical of tuyas, i.e. a basal succession or lithosome
570 composed of subaqueous, relatively coarse clastic lithofacies deposited from a variety of
571 sediment gravity flows (mainly hyperconcentrated flows) and sector collapses, and a
572 capping sequence of subaerial pāhoehoe lavas and tuff breccia that together comprise a
573 lava-fed delta. The bulk of the clastic lithofacies are crudely bedded relatively coarse lapilli
574 tuffs that probably formed during continuous-uprush episodes of rapid vertical aggradation
575 in a subaqueous tuff cone typical of Surtseyan cone construction; conversely, less common,
576 thinner sequences of thinner-bedded tuffs and finer lapilli tuffs were probably formed
577 during episodes of discrete tephra-jetting activity or during periods of quiescence allowing
578 redistribution of detritus from unstable volcano flanks (Smellie and Hole, 1997; Smellie and
579 Edwards, 2016). Snow Nunataks and Sims Island also represent tuyas in various stages of
580 construction and erosion, with many features similar to those seen in the Beethoven
581 Peninsula tuyas (Smellie, 1999; Smellie et al., 2009). By contrast, the multiple small outcrops
582 at Seal Nunataks are dominated by multiple dykes; other lithofacies are generally minor
583 apart from pillow lava, of which up to 150 m of vertical thickness is locally exposed above
584 the Larsen Ice Shelf. Additional lithofacies include subaqueously deposited lapilli tuffs
585 showing evidence for slope instability, similar to the basal subaqueous lithofacies at
586 Mussorgsky Peaks. The lithofacies appear to represent the basal lava-dominated (non-
587 explosive) pillow volcano cores of tuyas. The absence of lapilli tuffs associated with
588 explosive hydrovolcanic eruptions at most localities suggests that ambient pressures were
589 relatively high and were sufficient to suppress vesiculation consistent with either deep
590 water eruption or substantial contemporaneous ice thicknesses; minimum edifice heights of
591 c. 500-600 m are permissible, assuming the outcrops extend down to the present seafloor.
592 Proving that the outcrops were erupted subglacially is difficult but was based on the
593 presence of small patches of agglutinate resting on pillow lava at several localities. Such an
594 association is probably only possible if eruptions were subglacial and initially within a
595 meltwater-filled englacial vault. The vault must have drained at a later stage (presumably
596 initiating a jokulhlaup, for which there is no evidence preserved (as lithofacies)), resulting in
597 the subaerial exposure of the pillow lava pile and permitting the eruption to dry out,
598 transform to a magmatic eruption style and resulting in deposition of agglutinate and
599 clastogenic lavas. Such a sequence of events and association of lithofacies cannot occur in a
600 non-glacial (marine) setting and contemporary ice thicknesses > 600 m are therefore implied
601 (Smellie and Hole, 1997). The ice was also presumably wet based ice if it was hydraulically
602 lifted and basal drainage occurred. The outcrops at Beethoven Peninsula and Seal Nunataks
603 were used to examine and improve on the general model for subaqueous to emergent
604 Surtseyan volcanism associated with the construction of glaciovolcanic tuyas (Smellie and
605 Hole, 1997).

606 There is insufficient known about the small isolated volcanic outcrops at Henry Nunataks,
607 Merrick Mountains and Rydberg Peninsula to be confident of interpreting their eruptive

608 setting, although the eruptions were at least partly subaerial at Rydberg Peninsula and
609 Henry Nunataks. However, the small outcrop in the Merrick Mountains contains
610 hyaloclastite and may be glaciovolcanic (Rowley et al., 1990). Conversely, outcrops at Argo
611 Point (a scoria cone constructed on subaerial lavas) and Hornpipe Heights (dominated by
612 oxidised agglutinate and clastogenic lavas) were fully subaerial and presumably took place in
613 an absence of any significant local ice.

614 **Summary**

615 Late Neogene alkaline volcanic rocks form several monogenetic volcanic fields in the
616 Antarctic Peninsula. Some of the outcrops (Seal Nunataks) will be difficult to revisit now due
617 to contemporaneous ice shelf collapses and a consequent requirement for intensive
618 helicopter support of field parties. Isotopic dating shows that the volcanism is mainly Mio-
619 Pliocene in age (< 7.5 Ma). However, all of the published ages were determined by the
620 relatively imprecise K-Ar method and they should be repeated using the $^{40}\text{Ar}/^{39}\text{Ar}$ method
621 for greater reliability and accuracy, similar to recent investigations of other alkaline volcanic
622 fields in Antarctica (e.g. Chapters 3.2a, 5.1a, 5.2a and 5.3a). The Antarctic Peninsula
623 volcanism is post-subduction and thought to be causally related to the rise and
624 decompression melting of mantle through windows in the subducted slab following the
625 sequential (south to north) collision of a segmented spreading centre with the Peninsula
626 trench. However, there is no obvious correlation in timing between the initiation of volcanic
627 activity in the outcrops and cessation of subduction. This is an important problem that still
628 needs to be resolved for a fuller understanding of the genesis of the Neogene post-
629 subduction volcanism.

630 The outcrops occur as three principal types: rare scoria cones; glaciovolcanic sheet like
631 sequences; and tuyas. There are only two well-exposed examples of scoria cones: at Argo
632 Point and on Alexander Island at Hornpipe Heights. The sequences are relatively simple
633 accumulations of subaerially erupted scoria, agglutinate and clastogenic lavas. Other
634 possible examples include outcrops at Henry Nunataks and Rydberg Peninsula, which are
635 relicts of subaerial lava sequences whose sources and original morphologies are unclear.

636 Sheet-like sequences are restricted to a comparatively small area surrounding the summit of
637 Mt Pinafore and at Ravel Peak (Debussy Heights), in northern Alexander Island. They include
638 the oldest post-subduction volcanic outcrops in the Antarctic Peninsula south of James Ross
639 Island, extending back to c. 7.5 Ma. Their preservation, the variability of the lithofacies and
640 generally excellent exposed enabled them to be promoted as sequence holotypes for
641 glaciovolcanic sheet-like eruptions, originally called Mt Pinafore type. Only minimum coeval
642 ice thicknesses can be inferred for the outcrops, but they were probably thin (tens of
643 metres).

644 Tuyas are by far the commonest type of post-subduction Neogene volcanic edifice, being
645 characteristic of the Seal Nunataks, Beethoven Peninsula and Snow Nunataks volcanic fields.
646 The tuyas are the glaciovolcanic equivalents of subaqueous to emergent Surtseyan
647 volcanoes. Examples in each of the volcanic fields show different stages in the evolution of
648 tuyas, from the lava-dominated cores of pillow mounds, through explosively generated

649 tephra of a subaqueous tuff cone stage, to capping and pāhoehoe lava-fed deltas that were
650 responsible for laterally extending the edifices. The individual centres were erupted in
651 association with considerably greater ice thicknesses (hundreds of metres) than were
652 associated with the sheet-like sequences, and the lithofacies and architectural features
653 were gathered together in an illustrative general model for tuya construction. Investigations
654 of the post-subduction alkaline volcanism in the Antarctic Peninsula have thus been
655 important in establishing many of the diagnostic characteristics of glaciovolcanic sequences,
656 their styles of eruption and deducing the palaeoenvironmental implications.

657 **Acknowledgments**

658 The fieldwork on which this chapter is based was undertaken by MJH in 1985-1988. The
659 authors thank the British Antarctic Survey for originally supporting our project. Andy
660 Saunders is also thanked for additional information on the Argo Point outcrop, and we are
661 grateful to Janet Thomson for permission to publish her photograph of Mt Benkert.


662 **References**

- 663 Barker, P.F. 1982. The Cenozoic subduction history of the Pacific margin of the Antarctic
664 Peninsula: ridge crest—trench interactions. *Journal of the Geological Society, London*,
665 139, 787-801.
- 666 Barber, P.L., Barker, P.F. and Pankhurst, R.J. 1991. Dredged rocks from Powell Basin and the
667 South Orkney microcontinent. In Thomson, M.R.A., Crame, J.A. and Thomson, J.W. (eds)
668 *Geological evolution of Antarctica*. Cambridge University Press, Cambridge, pp. 361-367.
- 669 Bell, C.M. 1973. The geology of Beethoven Peninsula, south-western Alexander Island.
670 *British Antarctic Survey Bulletin*, 32, 75-83.
- 671 Burn, R.W. 1981. Early Tertiary calc-alkaline volcanism on Alexander Island. *British Antarctic*
672 *Survey Bulletin*, 53, 175-193.
- 673 Burn, R.W. 1984. The geology of the LeMay Group, Alexander Island. *British Antarctic Survey*
674 *Scientific Reports*, 109, 65 pp.
- 675 Burn, R.W. and Thomson, M.R.A. 1981. Late Cenozoic tillites associated with intraglacial
676 volcanic rocks, Lesser Antarctica. In Hambrey, M.J. and Harland, W.B. (eds) *Pre-*
677 *Pleistocene tillites: a record of Earth's glacial history*. Cambridge University Press,
678 Cambridge, pp. 199-203.
- 679 Care, B.W. 1980. The geology of Rothschild Island, north-west Alexander Island. *British*
680 *Antarctic Survey Bulletin*, 50, 87-112.
- 681 Del Valle, R.A., Fourcade, N.H. and Medina, F.A. 1983. Interpretación preliminar de las
682 edades K/Ar y de los análisis químicos de las rocas volcánicas y de los diques de los
683 nunataks Foca, Antártida. *Contribuciones del Instituto Antártico Argentino*, 287, 13 pp.
- 684 Fleet, M. 1968. The geology of the Oscar II Coast, Graham Land. *British Antarctic Survey*
685 *Scientific Reports*, 59, 46 pp.

- 686 González-Ferrán, O. 1983a. The Seal Nunataks: an active volcanic group on the Larsen Ice
687 Shelf, West Antarctica. In Oliver, R.L., James, P.R. and Jago, J.B. (eds) Antarctic earth
688 science. Australian Academy of Science, Canberra, pp. 334-337.
- 689 González-Ferrán, O. 1983b. The Larsen Rift: an active extension fracture in West Antarctica.
690 In Oliver, R.L., James, P.R. and Jago, J.B. (eds) Antarctic earth science. Australian Academy
691 of Science, Canberra, pp. 344-346.
- 692 Halpern, M. 1971. Evidence for Gondwanaland from a review of West Antarctic radiometric
693 ages. In Quam, L.O. (ed.) Research in the Antarctic. American Association for the
694 Advancement of Science, Washington, D.C., pp. 717-730.
- 695 Hathway, B. 2001. Sims Island: first data from a Pliocene alkaline volcanic centre in eastern
696 Ellsworth Land. *Antarctic Science*, 13, 87-88.
- 697 Hole, M.J. 1988. Post-subduction alkaline volcanism along the Antarctic Peninsula. *Journal of*
698 *the Geological Society, London*, 145, 985-989
- 699 Hole, M.J. 1990a. Geochemical evolution of Pliocene-Recent post-subduction alkalic basalts
700 from Seal Nunataks, Antarctic Peninsula: *Journal of Volcanology and Geothermal*
701 *Research*, 40, 149-167.
- 702 Hole, M.J. 1990b. Hornpipe Heights. In LeMasurier, W.E. and Thomson, J.W. (eds) *Volcanoes*
703 *of the Antarctic plate and southern oceans*. American Geophysical Union, Antarctic
704 *Research Series*, 48, pp. 271-272.
- 705 Hole, M.J. 1990c. Beethoven Peninsula. In LeMasurier, W.E. and Thomson, J.W. (eds)
706 *Volcanoes of the Antarctic plate and southern oceans*. American Geophysical Union,
707 *Antarctic Research Series*, 48, pp. 273-276.
- 708 Hole, M.J. and Thomson, J.W. 1990. Mount Pinafore—Debussy Heights. In LeMasurier, W.E.
709 and Thomson, J.W. (eds) *Volcanoes of the Antarctic plate and southern oceans*. American
710 *Geophysical Union, Antarctic Research Series*, 48, pp. 268-270.
- 711 Hole, M.J. and Larter, R.D. 1993. Trench-proximal volcanism following ridge crest-trench
712 collision along the Antarctic Peninsula. *Tectonics*, 12, 897-910.
- 713 Hole, M.J., Rogers, G., Saunders, A.D. and Storey, M. 1991. The relationship between alkalic
714 volcanism and slab-window formation. *Geology*, 19, 657-660.
- 715 Hole, M.J., Saunders, A.D., Rogers, G. and Sykes, M.A. 1995. The relationship between
716 alkaline magmatism, lithospheric extension and slab window formation along continental
717 destructive plate margins. In Smellie, J.L. (ed.) *Volcanism associated with extension at*
718 *consuming plate margins*. Geological Society, London, *Special Publication*, 81, pp. 265-
719 285.
- 720 Horne, P.R. and Thomson, M.R.A. 1967. Post-Aptian camptonite dykes in south-east
721 Alexander Island. *British Antarctic Survey Bulletin*, 14, 15-24.
- 722 Jonkers, H.A., Lirio, J.M., del Valle, R.A. and Kelley, S.P. 2002. Age and environment of
723 Miocene—Pliocene glaciomarine deposits, James Ross Island, Antarctica. *Geological*
724 *Magazine*, 139, 577-594.

- 725 Kyle, 1990. McMurdo Volcanic Group, western Ross Embayment. In: LeMasurier, W.E. and
726 Thomson, J.W. (eds) *Volcanoes of the Antarctic plate and southern oceans*. American
727 Geophysical Union, Antarctic Research Series, 48, pp. 19-25.
- 728 Larsen, C.A. 1894. The voyage of the Jason to the Antarctic regions. *Geographical Journal*, 4,
729 333-344.
- 730 Laudon, T.S. 1982. Geochemistry of Mesozoic and Cenozoic igneous rocks, eastern Ellsworth
731 Land. In Craddock, C. (ed.) *Antarctic geoscience*. University of Wisconsin Press, Madison,
732 pp. 775-785.
- 733 Lescinsky, D.T. and Sisson, T.W. 1998. Ridge-forming ice-bounded lava flows at Mount
734 Rainier, Washington. *Geology*, 26, 351-354.
- 735 Loughlin, S.C. 2002. Facies analysis of proximal subglacial and proglacial volcanoclastic
736 successions at the Eyjafjallajökull central volcano, southern Iceland. In Smellie, J.L. and
737 Chapman, M.G. (eds) *Volcano–Ice Interaction on Earth and Mars*. Geological Society of
738 London, Special Publication, 202, pp. 149–178.
- 739 Marensi, S.A., Casadío, S. and Santillana, S.N. 2010. Record of Late Miocene glacial deposits
740 on Isla Marambio (Seymour Island), Antarctic Peninsula. *Antarctic Science*, 22, 193-198.
- 741 Mathews, W.H., 1947. “Tuyas”: flat-topped volcanoes in northern British Columbia.
742 *American Journal of Science*, 245, 560-570.
- 743 McCarron, J.J. 1997. A unifying lithostratigraphy of late Cretaceous—early Tertiary fore-arc
744 volcanic sequences on Alexander Island, Antarctica. *Antarctic Science*, 9, 209-220.
- 745 McCarron, J.J. and Millar, I.L. 1997. The age and stratigraphy of fore-arc magmatism on
746 Alexander Island, Antarctica. *Geological Magazine*, 134, 507-522.
- 747 McCarron, J.J. and Smellie, J.L. 1998. Tectonic implications of fore-arc magmatism and
748 generation of high-magnesian andesites: Alexander Island, Antarctica. *Journal of the*
749 *Geological Society*, London, 155, 269-280.
- 750 Nelson, P.H.H. 1975. The James Ross Island Volcanic Group of northeast Graham Land.
751 *British Antarctic Survey Scientific Reports*, No. 54. 62 pp.
- 752 O’Neill, J.M. and Thomson, J.W. 1985. Tertiary mafic volcanic and volcanoclastic rocks of the
753 English Coast, Antarctica. *Antarctic Journal of the United States*, 20, 36-38.
- 754 Pankhurst, R. J., Riley, T. R., Fanning, C. M. and Kelley, S. P. 2000. Episodic silicic volcanism in
755 Patagonia and the Antarctic Peninsula: chronology of magmatism associated with break-
756 up of Gondwana. *Journal of Petrology*, 41, 605-625.
- 757 Pudsey, C.J. and Evans, J. 2001. First survey of Antarctic sub-ice shelf sediments reveals mid-
758 Holocene ice shelf retreat. *Geology*, 29, 787-790.
- 759 Renner, R.G.B. 1980. Gravity and magnetic surveys in Graham Land. *British Antarctic Survey*
760 *Scientific Reports*, 77, 99pp.
- 761 Renner, R.G.B., Dijkstra, B.J. and Martin, J.L. 1982. Aeromagnetic surveys over the Antarctic
762 Peninsula. In Craddock, C. (ed.) *Antarctic geoscience*. University of Wisconsin Press,
763 Madison, pp. 363-370.


- 764 Rex, D.C. 1970. Age of a camptonite dyke from south-east Alexander Island. *British Antarctic*
765 *Survey Bulletin*, 23, 103.
- 766 Rex, D.C. 1972. K-Ar age determinations on volcanic and associated rocks from the Antarctic
767 Peninsula and Dronning Maud Land. In Adie, R.J. (ed.) *Antarctic geology and geophysics*.
768 *Universitetsforlaget, Oslo*, pp. 133-136.
- 769 Rex, D.C. 1976. Geochronology in relation to the stratigraphy of the Antarctic Peninsula.
770 *British Antarctic Survey Bulletin*, 43, 49-58.
- 771 Riley T. R., Crame, J. A., Thomson, M. R. A. and Cantrill, D. J. 1997. Late Jurassic
772 (Kimmeridgian-Tithonian) macrofossil assemblage from Jason Peninsula, Graham Land:
773 evidence for a significant northward extension of the Latady Formation. *Antarctic*
774 *Science*, 9, 434-442.
- 775 Riley, T.R., Flowerdew, M.J., Hunter, M.A. and Whitehouse, M.J. 2010. Middle Jurassic
776 rhyolite volcanism of eastern Graham Land, Antarctic Peninsula: age correlations and
777 stratigraphic relationships. *Geological Magazine*, 147, 581-595.
- 778 Rowley, P.D. and Smellie, J.L. 1990. Southeastern Alexander Island. In LeMasurier, W.E. and
779 Thomson, J.W. (eds) *Volcanoes of the Antarctic plate and southern oceans*. American
780 *Geophysical Union, Antarctic Research Series*, 48, pp. 277-279.
- 781 Rowley, P.D. and Thomson, J.W. 1990. Rydberg Peninsula. In LeMasurier, W.E. and
782 Thomson, J.W. (eds) *Volcanoes of the Antarctic plate and southern oceans*. American
783 *Geophysical Union, Antarctic Research Series*, 48, pp. 280-282.
- 784 Rowley, P.D., Vennum, W.R. and Smellie, J.L. 1990. Merrick Mountains. In LeMasurier, W.E.
785 and Thomson, J.W. (eds) *Volcanoes of the Antarctic plate and southern oceans*. American
786 *Geophysical Union, Antarctic Research Series*, 48, pp. 296-297.
- 787 Saunders, A.D. 1982. Petrology and geochemistry of alkali-basalts from Jason Peninsula,
788 Oscar II Coast, Graham Land. *British Antarctic Survey Bulletin*, 55, 1-9.
- 789 Scarrow, J.H., Leat, P.T., Wareham, C.D. and Millar, I.L. 1998. Geochemistry of mafic dykes in
790 the Antarctic Peninsula continental margin batholith: a record of arc evolution.
791 *Contributions to Mineralogy and Petrology*, 131, 289-305.
- 792 Skilling, I.P. 1994. Evolution of an englacial volcano: Brown Bluff, Antarctica. *Bulletin of*
793 *Volcanology*, 56, 573-591.
- 794 Skilling, I.P. 2002. Basaltic pahoehoe lava-fed deltas: large-scale characteristics, clast
795 generation, emplacement processes and environmental discrimination. In Smellie, J.L.
796 and Chapman, M.G. (eds) *Volcano—ice interaction on Earth and Mars*. Geological
797 *Society, London, Special Publications*, 202, 91-113.
- 798 Smellie, J.L. 1987. Geochemistry and tectonic setting of alkaline volcanic rocks in the
799 Antarctic Peninsula: a review. *Journal of Volcanology and Geothermal Research*, 32,
800 269-85.
- 801 Smellie, J.L. 1990. Seal Nunataks. In LeMasurier, W.E. and Thomson, J.W. (eds) *Volcanoes of*
802 *the Antarctic plate and southern oceans*. American Geophysical Union, Antarctic
803 *Research Series*, 48, pp. 349-351.

- 804 Smellie, J.L. 1991. Middle—Late Jurassic volcanism on Jason Peninsula, Antarctic Peninsula,
805 and its relationship to the break-up of Gondwana. In Ulbrich, H. and Rocha Campos, A.C.
806 (eds) Gondwana seven proceedings. Instituto de Geociencias, Universidade de Sao Paulo,
807 pp. 685-699.
- 808 Smellie, J.L. 1999. Lithostratigraphy of Miocene-Recent, alkaline volcanic fields in the
809 Antarctic Peninsula and eastern Ellsworth Land. *Antarctic Science*, 11, 362-378.
- 810  Smellie, J.L. 2008. Basaltic subglacial sheet-like sequences: evidence for two types with
811 different implications for the inferred thickness of associated ice. *Earth-Science Reviews*,
812 88, 60-88.
- 813 Smellie, J.L. 2013 Quaternary volcanism: subglacial landforms. In Elias S.A. (ed.) Reference
814 module in *Earth Systems and Environmental Sciences*, from *The Encyclopedia of*
815 *Quaternary Science (Second Edition)*, Vol. 1. Elsevier, Amsterdam, pp. 780-802.
- 816 Smellie, J.L. 2018. Glaciovolcanism – a 21st century proxy for palaeo-ice. In Menzies, J. and
817 van der Meer, J.J.M. (eds) *Past Glacial Environments (sediments, forms and techniques)*,
818 2nd edition. Elsevier, Amsterdam, Netherlands, pp. 335-375.
- 819 Smellie J.L., Pankhurst, R.J., Hole, M.J. and Thomson, J.W. 1988. Age, distribution and
820 eruptive conditions of late Cenozoic alkaline volcanism in the Antarctic Peninsula and
821 eastern Ellsworth Land. *British Antarctic Survey Bulletin*, 80, 21-49.
- 822 Smellie J.L., Hole, M.J. and Nell, P.A.R. 1993. Late Miocene valley-confined subglacial
823 volcanism in northern Alexander Island, Antarctic Peninsula. *Bulletin of Volcanology*, 55,
824 273-288.
- 825 Smellie, J.L. and Skilling, I.P. 1994. Products of subglacial eruptions under different ice
826 thicknesses: two examples from Antarctica. *Sedimentary Geology*, 91, 115-129.
- 827 Smellie, J.L. and Hole, M.J. 1997. Products and processes in Pliocene-Recent, subaqueous to
828 emergent volcanism in the Antarctic Peninsula: examples of englacial Surtseyan volcano
829 construction. *Bulletin of Volcanology*, 58, No. 8, 628-646.
- 830 Smellie, J.L. McIntosh, W.C., Esser, R. and Fretwell, P. 2006a. The Cape Purvis volcano,
831 Dundee Island (northern Antarctic Peninsula): late Pleistocene age, eruptive processes
832 and implications for a glacial palaeoenvironment. *Antarctic Science*, 18, 399-408.
- 833 Smellie, J.L., McArthur, J.M., McIntosh, W.C. and Esser, R. 2006b. Late Neogene interglacial
834 events in the James Ross Island region, northern Antarctic Peninsula, dated by Ar/Ar and
835 Sr-isotope stratigraphy. *Palaeogeography, Palaeoclimatology, Palaeoecology*, 242, 169-
836 187.
- 837 Smellie, J.L., Johnson, J.S., McIntosh, W.C., Esser, R., Gudmundsson, M.T., Hambrey, M.J.
838 and van Wyk de Vries, B. 2008. Six million years of glacial history recorded in the James
839 Ross Island Volcanic Group, Antarctic Peninsula. *Palaeogeography, Palaeoclimatology,*
840 *Palaeoecology*, 260, 122-148.


- 841 Smellie, J.L., Haywood, A.M., Hillenbrand, C-D., Lunt, D.J. and Valdes, P.J. 2009. Nature of
842 the Antarctic Peninsula Ice Sheet during the Pliocene: geological evidence and modelling
843 results compared. *Earth-Science Reviews*, 94, 79-94.
- 844 Smellie, J.L., Johnson, J.S. and Nelson, A.E. 2013. Geological map of James Ross Island. 1.
845 James Ross Island Volcanic Group (1:125 000 scale). BAS GEOMAP 2 Series, Sheet 5,
846 British Antarctic Survey, Cambridge, UK. [available to download at:
847 <http://nora.nerc.ac.uk/506743/1/BAS%20GEOMAP%202%2C%20sheet%205%20-%20Geological%20map%20of%20James%20Ross%20Island%20-%20I%20-%20James%20Ross%20Island%20volcanic%20group.pdf>]
848
849
- 850 Smellie, J.L. and Edwards, B.E. 2016. Glaciovolcanism on Earth & Mars. Products, processes
851 and palaeoenvironmental significance. Cambridge University Press, 483 pp.
- 852 Thomson, J.W. and Kellogg, K.S. 1990. Henry Nunataks. In LeMasurier, W.E. and Thomson,
853 J.W. (eds) *Volcanoes of the Antarctic plate and southern oceans*. American Geophysical
854 Union, Antarctic Research Series, 48, pp. 294-295.
- 855 Thomson, J.W. and O'Neill, J.M. 1990. Snow Nunataks. In LeMasurier, W.E. and Thomson,
856 J.W. (eds) *Volcanoes of the Antarctic plate and southern oceans*. American Geophysical
857 Union, Antarctic Research Series, 48, pp. 283-285.
- 858 Walker, G.P.L. and Blake, D.H. 1966. The formation of a palagonite breccia mass beneath a
859 valley glacier in Iceland. *Journal of the Geological Society, London*, 122, 45–61.
- 860 White, J.D.L. and Houghton, B.F. 2006. Primary volcanoclastic rocks. *Geology*, 34, 677-680.

861

862 **Figures**

863 Figure 1  sketch maps of the Antarctic Peninsula and southern South America
864 illustrating the tectonic setting of slab-window development along the
865 Antarctic Peninsula between 15 Ma and present, with progressive
866 consumption of a spreading centre northwards with time. Triangle ornament
867 represents active subduction and double lines represent spreading ridge
868 segment. In (b), the collision times for each ridge segment are given on the
869 oceanward margin of the peninsula. Abbreviations: NAI, Northern Alexander
870 Island; SN, Seal Nunataks; JRI, James Ross Island; BS, Bransfield Strait. After
871 [Hole and Larter \(1993\)](#) and [Hole et al. \(1995\)](#).

872 Figure 2 (a) Perspective view of slab window growth with time, showing the
873 geographical location of the slab window-related basalts (red-coloured
874 trapezoids with K-Ar age adjacent). The ages of basalts in each of the
875 outcrops is also given. Note that volcanism in James Ross Island is not related
876 to a slab window and is discussed in Chapter 3.2a. After [Hole et al. \(1995\)](#). (b)
877 Plan view of slab window development over time along the Antarctic
878 Peninsula. The x-axis represents the palaeo-trench and the different
879 ornaments correspond to the amount of slab window formation associated
880 with each spreading ridge, the solid lines separating the ornaments being
881 'isochrons' for the slab window as a whole. It is assumed that the subducted

- 882 slab was planar, and the slab dip did not vary over time. See [Hole et al. \(1995\)](#)
883 for further explanation.
- 884 Figure 3 Map of the Antarctic Peninsula showing the locations of the late Neogene
885 volcanic fields (modified after [Smellie, 1999](#)). The two major volcanic groups
886 are also shown (grey dashed ellipses). Description of the Mt Haddington
887 Volcanic Field is included in Chapter 3.2a.
- 888 Figure 4 Maps showing the geology, isotopic ages and dyke trends of Seal Nunataks
889 (modified after [Smellie and Hole, 1997](#)).
- 890 Figure 5 Photomontage of field photos of Seal Nunataks & associated lithofacies. a)
891 view of Dalmann Nuntak looking north from Bull Nunatak with a tidal melt-
892 pool in the foreground. Despite the cone-like landform, no primary structure
893 is preserved and the nunatak is dominated by pillow basalt with a central
894 dyke zone. b) View looking southeast from Dalmann Nunatak with Åkerlundh
895 Nunatak on the left and Gray, Hertha and Castor nunataks from front to back,
896 respectively. c) Likely pillow lava at Dalmann Nunatak. d) Dyke zone on the
897 north flank of Larsen Nunatak. The majority of the nunatak is made of pillow
898 lava and the dykes are seen to terminate in the pillow lava pile at the summit
899 of the nunatak. e) Subaerial lava flows at Castor Nunatak overlying
900 subhorizontally bedded yellow-orange lapilli tuffs containing accretionary
901 lapilli. The lapilli tuffs are at approximately the same elevation as pillow lavas
902 at Larsen and Dalmann nunataks, suggesting that eruptions occurred under
903 varied ice thicknesses at different times. f) Broken slabs and homogenized
904 lapilli tuff at Bruce Nunatak. The structure suggests destabilization and local
905 fluidization of a weakly lithified stratified lapilli tuff sequence. The majority of
906 Bruce Nunatak is composed of pillow basalt.
- 907 Figure 6 Google Earth satellite view of the Argo Point scoria cone. Note the prominent
908 debris trail stretching for > 4 km northeast of the cone.
- 909 Figure 7  Maps showing the location of Neogene alkaline volcanic outcrops on
910 Alexander Island, and at Snow Nunataks and Merrick Mountains (modified
911 after [Smellie, 1999](#)).
- 912 Figure 8 Photomontage of field photos of glaciovolcanic sheet-like sequences near Mt
913 Pinafore, & associated lithofacies. a) View looking west towards exposures of
914 volcanic rocks at Mount Pinafore. They rest unconformably on steeply
915 dipping accretionary prism metasedimentary rocks (LeMay Group), which
916 make up much of the foreground. b) View of the 'Twin Peaks' locality on
917 Mount Pinafore (see Fig. 9, locality KG.2217, KG.3616) with the basal
918 unconformity with the underlying LeMay Group indicated. c) Irregular lava
919 lobes and pillow masses mingled with yellow-orange tuff breccia at the base
920 of a water-chilled lava low in the Mount Pinafore section. Several of the lava
921 masses show prominent chilled margins; the hammer is c. 40 cm long. d)
922 Well-bedded reddish-brown volcanic sandstones and fine conglomerates

- 923 overlying massive to poorly bedded, poorly sorted yellow-orange tuff breccia
 924 at the base of the Mount Pinafore section. Locality KG.2223 (Fig. 9). e) Poorly
 925 stratified grey diamictite overlain by yellow tuff breccia in irregular contact
 926 with overlying coeval tephrite lava. Note the prominent reaction front
 927 (yellow) caused by intense palagonitization within the tuff breccia. A small
 928 pillow-like lava mass is also present in the tuff breccia at the upper left of the
 929 image. Locality KG.3616 (Fig. 9). f) c. 75 m-thick pooled tephrite lava flow
 930 with a well-developed colonnade and entablature. The sloping apron at the
 931 base of the lava flow obscures outcrop of diamictite overlain by poorly seen
 932 volcanic sandstones. The diamictite contains abraded and partly striated
 933 cobbles and boulders of greenish volcanic rocks derived from the underlying
 934 calc-alkaline lava succession, together with numerous clasts of low-grade
 935 metasedimentary rocks of the LeMay Group. The lava contains numerous
 936 spinel peridotite xenoliths up to 25 cm in diameter. Locality KG.3609 (Fig. 9).
- 937 **Figure 9** Vertical profile sections and selected outcrop views of glaciovolcanic
 938 sequences in the Mt Pinafore Volcanic Field (after [Smellie et al., 1993](#), and
 939 [Smellie and Skilling, 1994](#)); Debussy Heights geology based on field notes of
 940 PAR Nell.
- 941 **Figure 10** Views of the subaerially erupted volcanic sequence and lithofacies at
 942 Hornpipe Hts. a) Red (oxidised) agglutinate, scoria and clastogenic lavas
 943 draped on a steep underlying slope composed of LeMay Group
 944 metasedimentary rocks. b) Aerial view of the Hornpipe Heights outcrop with
 945 the apron of red scoriaceous volcanoclastic rocks clearly visible. The outcrop is
 946 c. 1 km wide at its base. c) Beautifully preserved reddened basanite
 947 agglutinate. Black fine-grained lavas appear to be present towards the base
 948 of the sequence but close inspection reveals that they are fine-grained
 949 agglutinates with numerous internal chilled margins. Kaersutite megacrysts
 950 are common at this locality.
- 951 **Figure 11** Photomontage of field photographs of tuyas on Beethoven Peninsula and
 952 associated lithofacies. a) View of Mount Grieg (c. 600 m asl) from the
 953 southeast. Like other outcrops on Beethoven Peninsula, the lower part of the
 954 exposed sequence is composed of black pillow lava, hyaloclastite and bedded
 955 volcanoclastic rocks. They are capped by pillow basalt, tuff breccia and likely
 956 subaerial lavas, corresponding to a typical tuya sequence. Mt Greig has never
 957 been visited due to the impassable surrounding terrain. b) Mussorgsky Peak
 958 (c. 630 m asl) viewed from the north from a distance of ~750 m. The lower,
 959 orange-yellow part of the sequence is entirely volcanoclastic in origin (lapilli
 960 tuffs). The black caprock is composed of basal tuff breccia and pillow lavas
 961 overlain by subaerial pāhoehoe lava at the summit. At the extreme left, the
 962 poorly seen grey ridge contains a series of east—west-trending multiple
 963 dykes. c) Tuff breccia composed of intact and fragmented lava pillows and
 964 palagonite-altered sideromelane exposed at the base of the black caprock.
 965 The white fragment in the centre of the image is a partially melted xenolith of

966 arkose with a glassy vesicular rim (buchite). The hammer haft is c. 40 cm long.
 967 d) Diffusely bedded lapilli tuffs in the lower parts of the Mussorgsky Peaks
 968 outcrop. The lapilli tuffs are locally cross-bedded on a metre scale. The lens
 969 cap is at extreme left is 52 mm in diameter. e) Tuff breccia derived from a
 970 collapsed pillow lava pile overlying possible lapilli tuff (yellow) at Gluck Peak
 971 (locality KG.3627). Unusually for Beethoven Peninsula, the pillows are highly
 972 vesicular, even in their chilled margins. Plagioclase phenocrysts are also
 973 clearly visible in hand specimens and are a rarity on Beethoven Peninsula.
 974 The width of the field of view is ~5m. f) Diffusely stratified and thin-bedded
 975 lapilli tuffs in the lower part of the Mussorgsky Peaks section. The thin dark
 976 brown beds are very fine-grained palagonite tuff, offset by syn-sedimentary
 977 faulting possibly related to large-scale slumping seen elsewhere on the
 978 outcrop. Some palagonite tuff has been mobilized and injected along near-
 979 vertical fractures in the centre of the image. The width of the field of view is
 980 c. 20m.

981 Figure 12 Photograph of Sims Island and geological interpretation (based on [Hathway,](#)
 982 [2001](#)).

983 Figure 13 Photograph of Mt Benkert, looking north. The sequence is composed of
 984 subaqueously erupted and emplaced basalt pillow lava, tuff breccia and
 985 orange-brown lapilli tuff. It is crossed by several very large convex-down
 986 channel-like structures caused by repeated coeval slumping events (slump-
 987 scar surfaces). The cliff is c. 350 m high. The red ring encloses a figure on a
 988 skidoo. Image: Janet Thomson.

989 Figure 14 Vertical profile logs & idealised cross sections for tuyas based on examples in
 990 Beethoven Peninsula and Seal Nunataks volcanic fields; modified after
 991 [Smellie and Hole \(1997\)](#). True-scale cross sections are also shown, with the
 992 major edifice-building stages numbered (1 – pillow mound; 2 – subaqueous
 993 tuff cone stage (mainly vertical aggradation); 3 – subaerial lava-fed delta
 994 stage (mainly lateral progradation)); the grey shaded boxes represent the
 995 extent of the preserved deposits in each volcanic field. Note that the Seal
 996 Nunataks examples show no evidence for a late lava-fed delta phase; instead,
 997 coeval (melt)water levels appear to have collapsed, probably by sudden
 998 subglacial discharge (jökulhaup(s)), and the subaqueous lithofacies (pillow
 999 lava, lapilli tuff) are draped by subaerial lithofacies (lava, agglutinate).

1000

1001 Tables

1002 Table 1 Outline stratigraphy of late Neogene, post-subduction, alkaline volcanic
 1003 outcrops in the Antarctic Peninsula.

1004 Table 2 Summary of published isotopic ages for post-subduction, slab-window-
 1005 related volcanic rocks in the Antarctic Peninsula.



THIS TABLE CAN BE DOWNLOADED FROM THE PDF TO VIEW MORE EASILY

Table 1. Outline stratigraphy of late Neogene alkaline volcanic outcrops in the Antarctic Peninsula

Volcanic Field	Principal localities included	Age (Ma)	Comments	Key references
JAMES ROSS ISLAND VOLCANIC GROUP				
Mt Haddington Volcanic Field	James Ross Island; islands in Prince Gustav Channel & Antarctic Sound; Tabarin Peninsula and southeastern Graham Land; Dundee Island; Paulet Island	6.25-0.08 (in situ outcrops); 12.4 and 9.2 for clasts in diamicts; essentially pristine scoria cones on eastern Mt Haddington suggests that volcanic field may still be active	Outcrops largely 'layer-cake' (mainly extensive superimposed lava-fed deltas) and, uniquely for Neogene volcanism in the region, lend themselves to a formal lithostratigraphy; 29 rock formations are defined (see Chapter 3.2a); compositionally and in lithofacies identical to other alkaline volcanic outcrops in the region but the volcanism probably overlaps geographically & in time with subduction at the South Shetland Trench and is therefore not 'post-subduction'	Nelson, 1975; Skilling, 1994; Smellie & Skilling, 1994; Jonkers et al., 2002; Smellie et al., 2006a,b, 2008, 2013; Marensi et al., 2010
Seal Nunataks Volcanic Field	Lindenberg Island; Larsen Nunatak; Murdoch Nunatak; Donald Nunatak; Akerlunth Nunatak; Evensen Nunatak; Dallmann Nunatak; Bruce Nunatak; Bull Nunatak; Gray Nunatak; Castor Nunatak; Christensen Nunatak; Oceana Nunatak; Pollux Nunatak; Argo Point	4.0- < 0.1		del Valle et al., 1983; Hole, 1990a; Smellie, 1999
BELLINGSHAUSEN SEA VOLCANIC GROUP				
Mt Pinafore Volcanic Field	Mt Pinafore summit and southwestern ridges (3 outcrops); Ravel Peak (Debussy Heights); Hornpipe Heights (all northern Alexander Island); Overton Peak (Rothschild Island)	7.7-5.4; younger age of 3.9 is probably unreliable		Care, 1980; Smellie et al., 1993
Beethoven Peninsula Volcanic Field	Mussorgsky Peaks; Mt Liszt; Mt Grieg; Mt Strauss; Gluck Peak; probably Mt Schumann, Chopin Hill, Mt Lee (all southwestern Alexander Island)	only two published ages: 2.5 and <0.1	Mt Grieg, Schumann, Chopin Hill and Mt Lee outcrops unvisited; good exposures at Mt Grieg observed by binocular	Hole, 1990c; Smellie and Hole, 1997
Snow Nunataks Volcanic Field	Espenchied Nunatak; Mt McCann; Mt Thornton; Mt Benkert; Sims Island; Rydberg Peninsula (southwestern Palmer Land)	4.7-1.6; an older age of 20 is probably unreliable		Rowley and Thomson, 1990; O'Neil and Thomson, 1990; Smellie, 1999; Hathway, 2001; Smellie et al., 2009
Merrick Mountains Volcanic Field	Henry Nunataks & outcrop west of Eaton Nunatak (southern Palmer Land)	6		Halpern, 1971; Rowley et al., 1990; Smellie, 1999

THIS TABLE CAN BE DOWNLOADED FROM THE PDF TO VIEW MORE EASILY

Table 2. Summary of published isotopic ages for post-subduction, slab-window-related volcanic rocks in the Antarctic Peninsula

Sample	Locality	Dated lithologies	Age (Ma)	error (Ma)	Method	Reference	Notes
Seal Nunataks							
D.4105.1	Akerlundh Nunatak	lava	< 0.1		K-Ar	Rex, 1972, 1976	published age modified by Smellie et al., 1988
D.4114.1	Larsen Nunatak	lava	< 0.1		K-Ar	Rex, 1972, 1976	published age modified by Smellie et al., 1988
D.727.2	Oceana Nunatak	lava	< 0.1		K-Ar	Rex, 1972, 1976	published age modified by Smellie et al., 1988
D.727.3	Oceana Nunatak	lava	< 0.1		K-Ar	Rex, 1972, 1976	published age modified by Smellie et al., 1988
41178/101	Akerlundh Nunatak	n.r.	0.7	0.3	K-Ar	del Valle et al., 1983	
141178/21	Arctowski Nunatak	n.r.	1.4	0.3	K-Ar	del Valle et al., 1983	
41178/102	Bruce Nunatak	n.r.	1.5	0.5	K-Ar	del Valle et al., 1983	
	Christensen Nunatak	n.r.	0.7	0.3	K-Ar	del Valle et al., 1983	
81178/5	Donald Nunatak	n.r.	< 0.2		K-Ar	del Valle et al., 1983	
201178/10	Evensen Nunatak	n.r.	1.4	0.3	K-Ar	del Valle et al., 1983	
201178/11	Evensen Nunatak	n.r.	4.0	1	K-Ar	del Valle et al., 1983	
141178/12	Gray Nunatak	n.r.	< 0.2		K-Ar	del Valle et al., 1983	
31178	Larsen Nunatak	n.r.	1.5	0.5	K-Ar	del Valle et al., 1983	
1178/10	Oceana Nunatak	n.r.	2.8	0.5	K-Ar	del Valle et al., 1983	
Jason Peninsula							
R.217.7	Argo Point	lava	1.0	0.3	K-Ar	Smellie et al., 1988	
R.217.7	Argo Point	lava	0.8	0.1	K-Ar	Smellie et al., 1988	
R.218.3	c. 37 km west of Argo Point	hematite-coated intrusion	1.6	0.5	K-Ar	Smellie et al., 1988	age unreliable; rock probably much older & unrelated to the post-subduction volcanism
R.218.3	c. 37 km west of Argo Point	hematite-coated intrusion	1.3	0.3	K-Ar	Smellie et al., 1988	age unreliable; rock probably much older & unrelated to the post-subduction volcanism
Alexander Island							
KG.2217.16	Mt Pinafore area	lava	3.9	0.4	K-Ar	Smellie et al., 1988, 1993	age probably unreliable (too young?)
KG.2217.14	Mt Pinafore area	lava	5.4	0.3	K-Ar	Smellie et al., 1988, 1993	
KG.2217.13	Mt Pinafore area	lava	6.0	0.2	K-Ar	Smellie et al., 1988, 1993	
KG.2217.13	Mt Pinafore area	lava	6.2	0.3	K-Ar	Smellie et al., 1988, 1993	
KG.2223.4	Mt Pinafore area	lava	6.9	0.2	K-Ar	Smellie et al., 1988, 1993	
KG.2223.3	Mt Pinafore area	lava	7.1	0.4	K-Ar	Smellie et al., 1988, 1993	
KG.2230.1	Mt Pinafore area	lava	7.7	0.6	K-Ar	Smellie et al., 1988, 1993	
KG.2230.1	Mt Pinafore area	lava	7.6	0.6	K-Ar	Smellie et al., 1988, 1993	
KG.2230.1	Mt Pinafore area	lava	7.3	0.4	K-Ar	Smellie et al., 1988, 1993	
KG.2431.5	Mt Pinafore area	lava	6.0	0.2	K-Ar	Smellie et al., 1988, 1993	
KG.2431.5	Mt Pinafore area	lava	6.3	0.2	K-Ar	Smellie et al., 1988, 1993	
KG.3619.4	Rothschild Island	lava	5.4	0.7	K-Ar	Smellie et al., 1988, 1993	
KG.3612.5	Hornpipe Heights	lava	2.5	0.8	K-Ar	Smellie et al., 1988, 1993	
KG.3608.9	Hornpipe Heights	lava	2.7	0.2	K-Ar	Smellie et al., 1988, 1993	
n.r.	Mussorgsky Peaks, Beethoven Peninsula	lava pillow	2.5	n.r.	K-Ar	Hole, 1990c	no analytical details
n.r.	Gluck Peak, Beethoven Peninsula	lava pillow	< 1	n.r.	K-Ar	Hole, 1990c	no analytical details
Snow Nunataks							
n.r.	Mt McCann	n.r.	20	n.r.	K-Ar	Smellie et al., 2009	unpublished age of JW Thomson; no analytical details; age may be unreliable
n.r.	Mt Benkert	n.r.	4.7	n.r.	K-Ar	Smellie et al., 2009	unpublished age of JW Thomson; no analytical details
n.r.	Mt Benkert	n.r.	4.6	n.r.	K-Ar	Smellie et al., 2009	unpublished age of JW Thomson; no analytical details
n.r.	Mt Thornton	n.r.	1.7	n.r.	K-Ar	Smellie et al., 2009	unpublished age of JW Thomson; no analytical details
n.r.	Mt Thornton	n.r.	1.6	n.r.	K-Ar	Smellie et al., 2009	unpublished age of JW Thomson; no analytical details
Sims Island							
R.6801.4	south tip of island	basaltic intrusion	3.46	1.2	Ar-Ar	Hathway, 2001	
R.6801.5	south tip of island	basaltic intrusion	2.3	0.54	Ar-Ar	Hathway, 2001	The younger age is regarded as the more reliable
Merrick Mountains							
		basalt	6	n.r.	K-Ar	Halpern, 1971	Reliability uncertain; no analytical details
n.r. - not recorded							

